Pressure-Tuned Topological Phases in Kagome Magnets (Gd, Tb)V_6Sn_6

X. M. Kong [1], *X. F. Yang* [1], *W. Xia* [2], *C.Y. Pei* [2], *Y. F. Guo* [2], *S. Y. Li* [1,*]

1. State Key Laboratory of Surface Physics and Department of Physics, Fudan University, Shanghai 200438, China
2. School of Physical Science and Technology, ShanghaiTech University, Shanghai 201210, China

Introduction

As one of the origins of novel phenomena encompassing quantum magnetism, a kagome lattice has played a key role for realizing and tuning novel electronic states, owing to its unique lattice geometry and band structure.

RV_6Sn_6 (R = rare-earth element) is a newly discovered kagome family, which is isostructural to $TbMn_6Sn_6$ structural prototype but the kagome layer composed of V atoms is nonmagnetic. For magnetic R-triangular lattice (R = Gd-Tm), the segregated magnetic layer not only permits a direct tunability for nonmagnetic kagome layer below the magnetic transition temperature T_m, but also obviates the complex magnetic configurations in RMn_6Sn_6 family because of a pristine Mn-kagome lattice.

Method

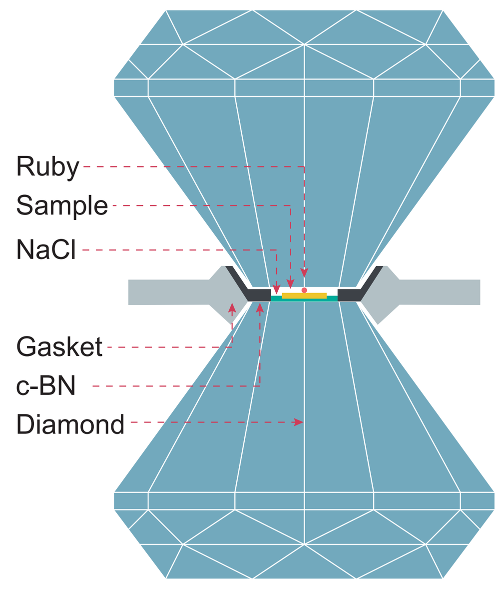

High-pressure electric transport measurements were performed in a diamond anvil cell (DAC) made of BeCu alloy with NaCl powder as the pressure transmitting medium. A mixture of c-BN powder and epoxy is adopted as the insulating layer. The pressures are determined by the ruby luminescence method.

The four-probe method and Van Der Pauw method are applied for the transverse magnetoresistance and Hall resistance measurements, respectively.

Longitudinal resistivity of (Gd, Tb)V_6Sn_6 at different pressures

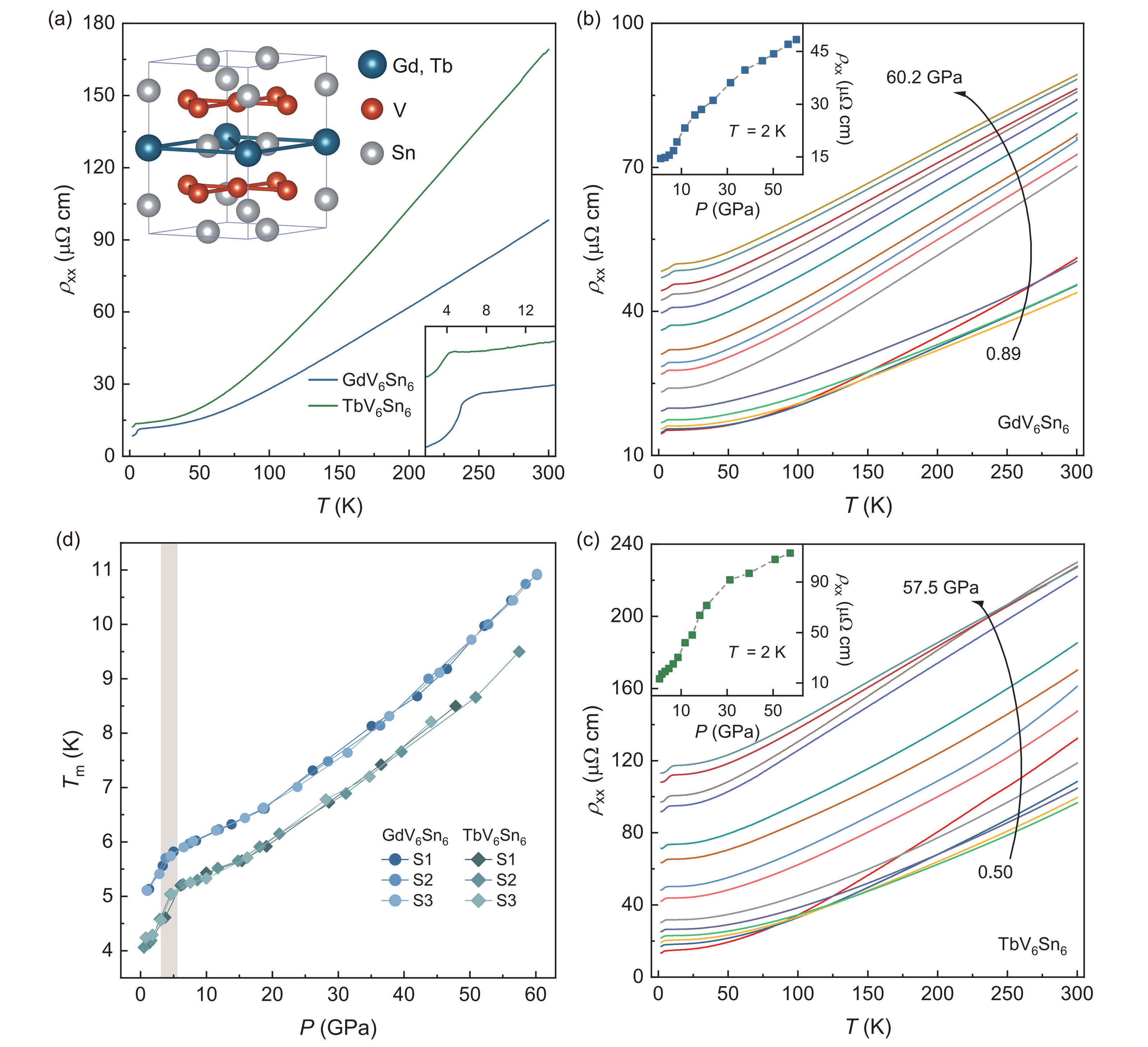

(a) Longitudinal resistivity ρ_{xx} as a function of temperature T at ambient pressure. Insets: crystal structure of (Gd, Tb)V_6Sn_6 and closeup of ρ_{xx} at T = 2 K. (b), (c) $\rho_{xx}(T)$ curves under various pressures. Insets: resistivity under different pressure at T = 2 K. (d) Pressure dependence of magnetic transition temperature T_m.

Pressure tuned magnetotransports of (Gd, Tb)V_6Sn_6

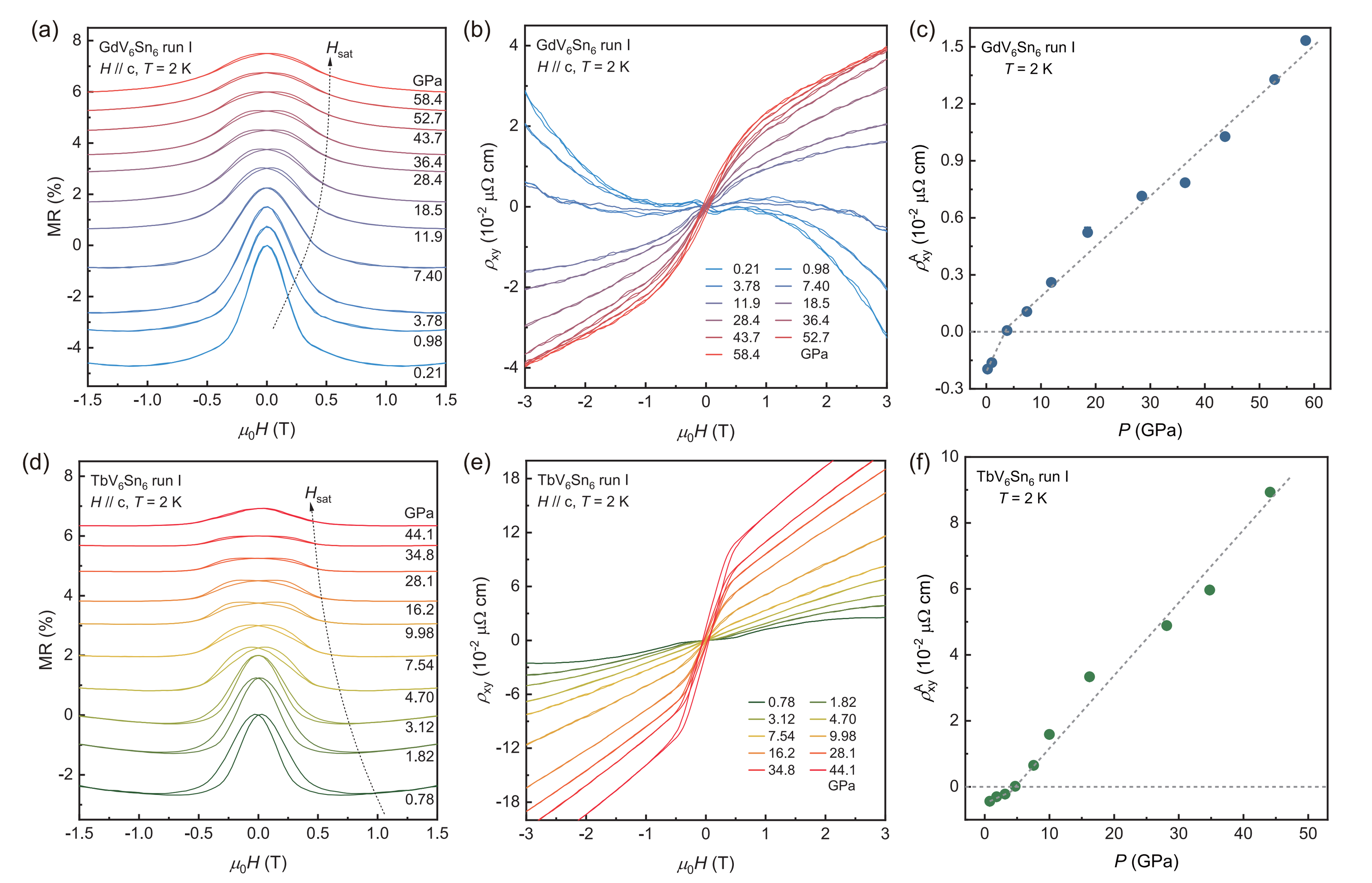

(a), (d) Field dependence of transverse magnetoresistivity (MR) of GdV_6Sn_6 and TbV_6Sn_6 under different pressure at T = 2 K. (b), (e) Hall resistivity ρ_{xy} under varying pressures at T = 2 K. (c), (f) Anomalous Hall resistivity ρ^A_{xy} as a function of pressure, which is derived from (b) and (e), respectively.

Temperature-dependent AHE of (Gd, Tb)V_6Sn_6 under pressure

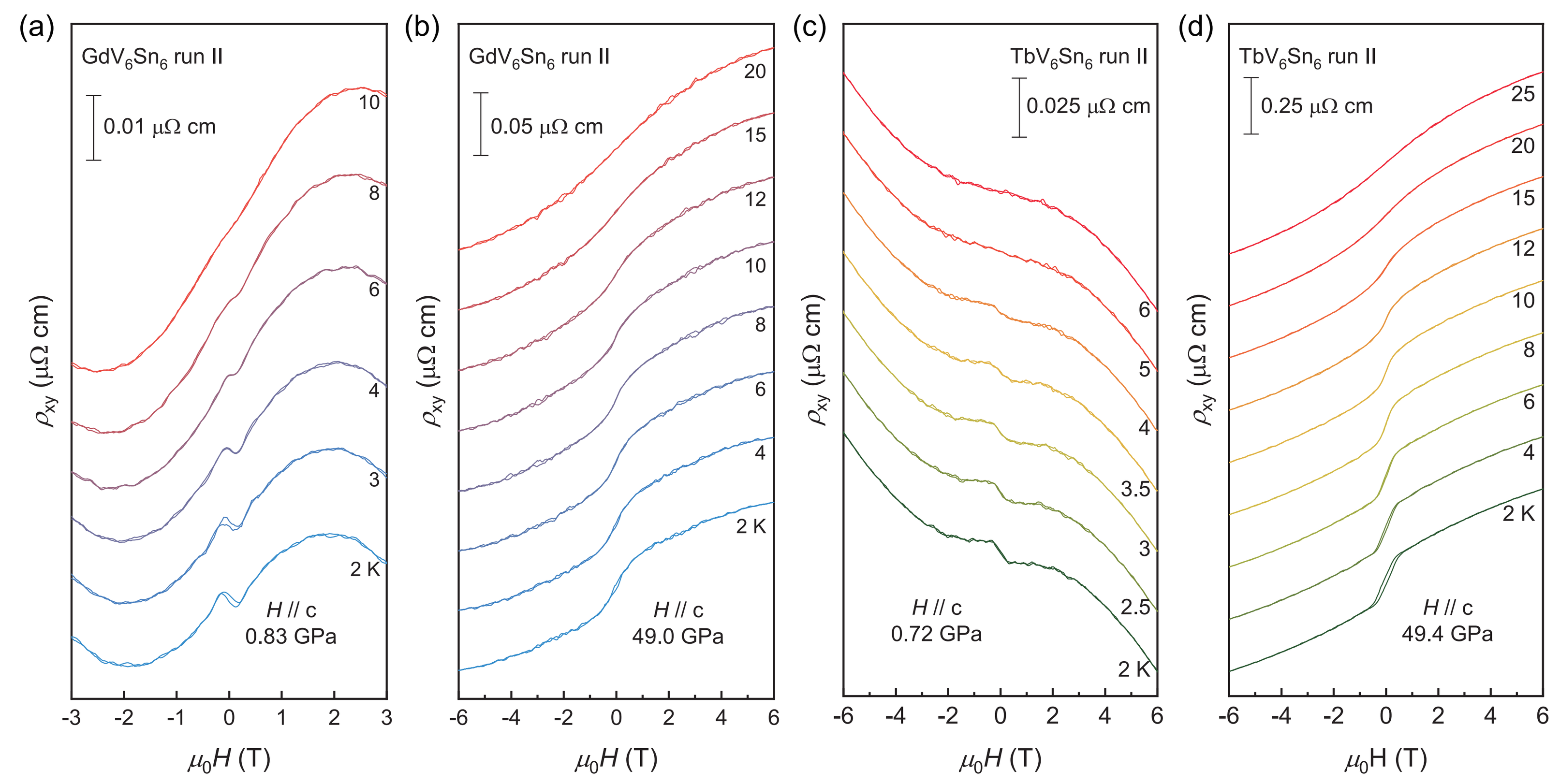

(a)-(d) ρ_{xy} versus $\mu_0 H$ at virous temperatures. Both of samples exhibit a positive anomalous Hall effect (AHE) under high pressure, while low-pressure AHE responds oppositely. The negative AHE is robust although the low-pressure ρ_{xy} of GdV_6Sn_6 represents another behavior against bulk or other batches in the range of $\mu_0 H$ = ±2 T.

Phase diagram and TYJ model fittings for (Gd, Tb)V_6Sn_6

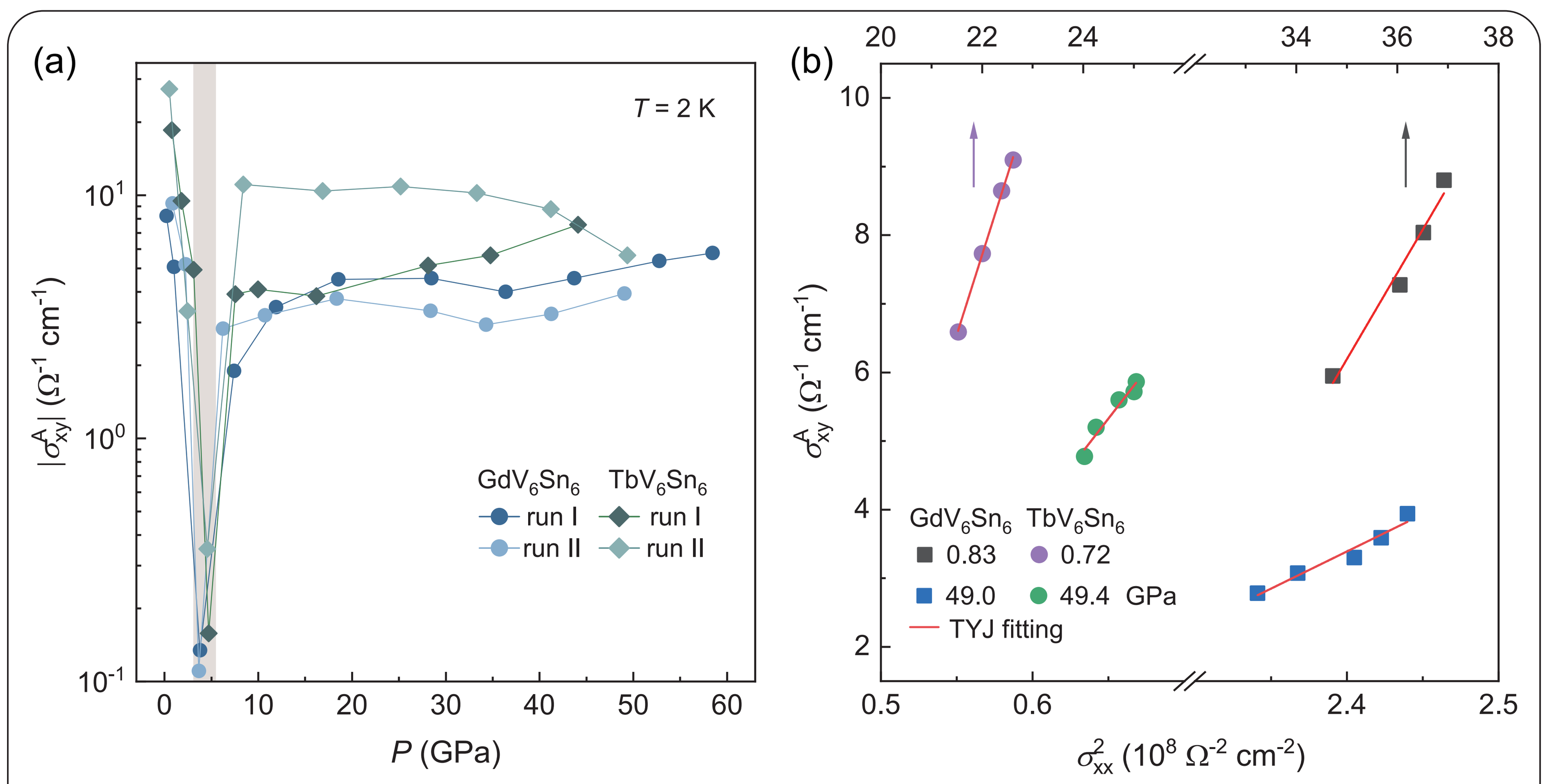

(a) Phase diagram of GdV_6Sn_6 and TbV_6Sn_6 with pressure. Beige shaded area highlights the anomaly of anomalous Hall conductivity σ^A_{xy} at T = 2 K crossing the critical pressures. (b) Fittings of σ^2_{xx} dependence of σ^A_{xy} using TYJ model (PRL 103, 087206 (2009)) for GdV_6Sn_6 and TbV_6Sn_6. All of well linear relationships reflect the pressure-induced AHE can mainly result from the intrinsic effect of the Berry curvature.

Conclusions

- In GdV_6Sn_6 and TbV_6Sn_6, we observe two pressure-induced anomalous Hall effect (AHE) features: an unusual suppression (below critical pressure) and a progressive enhancement (above critical pressure).
- Based on the TYJ model, both AHE features are mainly attributed to the intrinsic contribution of the Berry curvature. The AHE-weakened and AHE-enhanced regimes indicate that two distinct modulations of topological bands before and after the critical pressure.